Multimode Oscillation and Mode Competition in High-Frequency Gyrotrons

KENNETH E. KREISCHER, RICHARD J. TEMKIN, HAROLD R. FETTERMAN, SENIOR MEMBER IEEE, AND WILLIAM J. MULLIGAN

Abstract—**Stable operation in a single mode is an important goal of high-power gyrotrons. Both multimoding and switching into unwanted modes can lead to lower efficiency and undesirable heating of components not designed to accommodate parasitic modes. We have extensively studied mode behavior in a pulsed 100-kW, 140-GHz gyrotron using a variety of mixing techniques. As a result, a number of multimoding regions have been identified. Two possible explanations are presented. If the ratio of beam thickness to cavity radius is relatively large, different parts of the beam can excite different modes. Secondly, it can be shown theoretically that, under certain conditions, the presence of one mode can enlarge the excitation region of a neighboring, parasitic mode by favorably prebunching the beam. Experimental evidence strongly supports this latter interpretation. To our knowledge, this is the first use of mixing techniques in conjunction with the study of gyrotron operation. These diagnostic methods are important because they can conclusively identify the presence of parasitic modes, even when these modes are weakly excited.**

I. INTRODUCTION

THE GYROTRON has been demonstrated to be an efficient, high-power source of millimeter radiation. It is being utilized in a variety of applications, including electron-cyclotron heating in fusion experiments. Recent experiments have led to significant improvements in both power and frequency. Pulsed devices with powers in excess of 100 kW have been built at frequencies of 28 [1], 35 [2], [3], 45 [4], 60 [5], [6], 86 [7], 100 [4], and 140 [8] GHz. In addition, high-power CW operation has been achieved at 28 and 60 GHz [5].

As gyrotron technology is extended to higher power and frequency, it becomes necessary to use oversized cavities and to operate in higher order modes. The primary reason for this is ohmic heating of the cavity walls due to the RF field confined in the resonator. In order to avoid damaging these walls, this heat flux must be kept below some critical value, typically 1 or 2 kW/cm^2. As the gyrotron cavity becomes larger, the density of modes that it can support rises, increasing the likelihood of exciting parasitic modes, or of having multimode oscillations. One of the primary goals of gyrotron research is to better understand how the electron beam can interact with a variety of competing modes, so that techniques can be developed that will ensure stable, single-mode operation.

Manuscript received February 28, 1983; revised August 4, 1983. This work was supported in part by U.S.D.O.E. under Contract DE-AC02-78ET-51013.

K. E. Kreischer, R. J. Temkin, and W. J. Mulligan are with the Plasma Fusion Center, Massachusetts Institute of Technology, Cambridge, MA 02139.

H. R. Fetterman is with the Electrical Engineering Department, University of California, Los Angeles, CA 90024.

There are a variety of reasons why multimode oscillations should be avoided when operating a high-power gyrotron. If the tube is operating in the desired mode and a parasitic mode is accidentally excited, the efficiency will generally decrease. This is due primarily to adverse bunching of the electron beam by the parasitic mode, reducing the transfer of energy to the mode of interest. Under certain conditions, for example, when competing modes each couple with different parts of the beam, multimoding may result in higher efficiency [9] (see discussion on beam thickness later in this paper). However, multimoding can cause other problems, especially if components of the gyrotron system are designed for one particular mode. Modes excited at the wrong frequency may become trapped inside the gyrotron (e.g., by the window), leading to excessive localized heating. External components, such as mode filters, converters, and the transmission system, may also be mode dependent. In addition, if the gyrotron is designed to operate in a symmetric mode (TE_{mpq}, $m = 0$) and an asymmetric mode is excited, this may cause the wall heat flux to become excessive, resulting in damage to the resonator. This is particularly problematic for surface modes (modes with $(1 - m^2/\nu_{mp}^2) \ll 1$, where ν_{mp} is the pth root of $dJ_m(y)/dy = 0$, such as whispering-gallery modes) since the RF power is localized near the wall, resulting in relatively high wall losses. Thus, it becomes very important to understand under what conditions multimode oscillations will occur, and to develop techniques for their detection.

Past studies of multimoding have concentrated primarily on theoretical studies of the interaction between the beam and RF field, and on methods of mode suppression. A comprehensive review of multimode theory is given by Nusinovich [10]. This includes discussions on such topics as mode stability, nonlinear excitation of parasitic modes, and mode locking. Moiseev and Nusinovich [11] outline the equations governing the dynamics of the gyrotron, and use them to analyze its behavior when two modes with close frequencies can resonate in the cavity. In an earlier paper [12], we describe the mode spectrum of a gyrotron oscillator, and show how the startup procedure of a pulsed device can strongly influence which modes are excited. Dialetis and Chu [13] explain how an unstable, two-mode state can lead to mode jumping. Finally, in a paper by Nusinovich [14], the modifications resulting from a more realistic description of the beam and resonator are presented. This includes the effects of a beam velocity spread, a finite beam thickness, and the study of a cavity with a fixed (i.e.,

0018-9480/84/0500-0481$01.00 ©1984 IEEE

nonrotating) azimuthal field structure (e.g., the field of a slotted cavity).

In the area of mode suppression, Vomvoridis [15] uses a self-consistent nonlinear analysis to determine the conditions under which suppression occurs. An early paper by Vlasov [16] discusses how profiling the cavity wall can modify the axial field profile and lead to desirable thinning of the mode spectrum. Zapevalov [17] describes a second harmonic experiment in which mode selection techniques were utilized, resulting in stable, high-power operation. The two techniques that proved the most useful were insertion of dielectric pieces to modify the RF field, and profiling of the magnetic field. Ganguly and Chu [18] discuss the mode selection properties of a two-cavity gyroklystron, in which a low-order mode in the bunching cavity is coupled to a high-order mode in the output cavity by the beam. Other versions of the concept have also been analyzed in earlier papers [19]. Carmel *et al.* [20] describe the characteristics of an oscillator designed to operate in the TE_{041} mode, concentrating primarily on methods to suppress the neighboring parasitic mode TE_{241}. Finally, a review of other mode selection techniques is provided by Gaponov *et al.* [7].

In this paper, a variety of sensitive diagnostics utilizing mixer techniques will be discussed. Use of mixer diodes allows one to detect a weak second signal in the presence of a strong emission signal. The paper will be organized in the following manner. In Section II, a description of the gyrotron will be given, and the mixer technology used to diagnose multimoding will be examined. In Section III, the operational characteristics of the oscillator will be described. A map of the modes excited as a function of the magnetic field B_o and the cathode voltage V_c will be presented, showing regions of single and multimode oscillations. In Section IV, the experimental data will be compared with theoretical predictions. It is found that linear theory successfully predicts regions of single-mode oscillation, but that a nonlinear description is required for multimoding. The method of successive approximations, formulated by Nusinovich [10] to analyze the dynamics of a gyrotron, will be employed to calculate the starting current of a parasitic mode when another mode already exists in the cavity. In Section V, conclusions reached based on these experimental and theoretical studies will be reviewed.

II. Description of Experiment

The MIT gyrotron [8] has been operational since early 1982 and has been tested over a wide range of parameters. The magnetic field has been varied from 40 to 70 kG, the cathode voltage from 23 to 80 kV, and the beam current up to 8 A. An output power of 130 kW was obtained at 140 GHz in the TE_{031} mode, and by carefully adjusting the field single-mode emission was possible during the pulse flattop, which lasts about 1 μs. This represents a total efficiency of 24 percent at the highest current. Efficiencies approaching 28 percent have been obtained at lower currents in this mode. Efficiencies as high as 36 percent have been obtained in the TE_{231} mode at 137 GHz. This gyrotron is characterized by a number of unique features, including the interaction of the beam with the second radial maximum of the RF field, and operation of a magnetron injection gun into a magnetic compression region with a mirror ratio of 25.

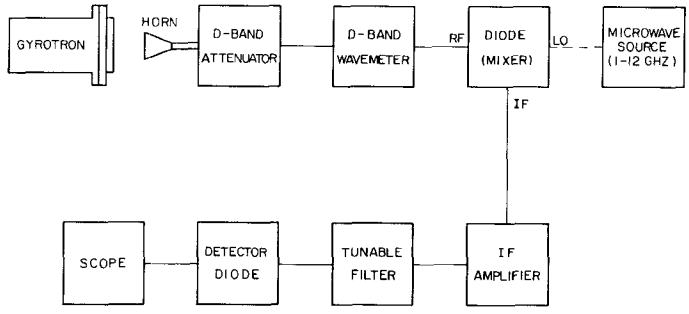

Fig. 1. A schematic of the mixer-diode diagnostic system used to analyze RF emission from the 140-GHz gyrotron.

TABLE I
Mixer Techniques

Measured Quantity	Resonance Condition	Advantage	Disadvantage
ω in a fundamental mixer	$\pm\omega_{IF} = \omega_{LO} - \omega$	Accurate ω measurement	Expensive, high frequency LO required
ω in a harmonic mixer	$\pm\omega_{IF} = n\omega_{LO} - \omega$	Low frequency LO is more available	Higher input power required
$\Delta\omega$ in a harmonic mixer without an LO	$\pm\omega_{IF} = m\Delta\omega$	Data easy to interpret	Loss of sensitivity when $\omega_{IF} \geq 5$ GHz
$\Delta\omega$ in a harmonic mixer with an LO	$\pm\omega_{IF} = n\omega_{LO} - m\Delta\omega$	Greater sensitivity	Data interpretation more difficult

n and m are arbitrary integers

A schematic of the mixer-diode system used to detect multimoding in this device is shown in Fig. 1. The RF power that is generated in the resonator is carried by oversized copper waveguide to a Corning 7940 fused-quartz window 0.554 cm thick. After transmission through the window, the radiation is broadcast into free space. At a distance of 50 cm, a portion of this signal is collected by a horn and passes through an attenuator and a wavemeter. The radiation then enters the RF port of the mixer diode. The output signal from the IF port is amplified and sent through a tunable filter to a detector diode and scope.

Both commercial mixer diodes made by Hughes, and a Lincoln Lab corner-cube diode [21], were utilized in this system. These mixer diodes were operated both with and without a local oscillator (LO). Use of an LO increases sensitivity and allows one to detect weak input signals. A variety of LO sources in the 1–12-GHz range were used, including a Wavetek 907A for 7.0–12.4 GHz, and an HP 8620 for lower frequencies. When the system was operated with an LO, the IF filter was set at 100 ± 50 MHz, and the LO was swept. When no LO was used, a YIG filter was electronically tuned to find resonance signals generated by the mixer.

In Table I, a summary of diagnostic techniques using mixer technology is shown. The type of measurement is given in the first column, the resonance condition of the diode is in the next column, and the advantages and

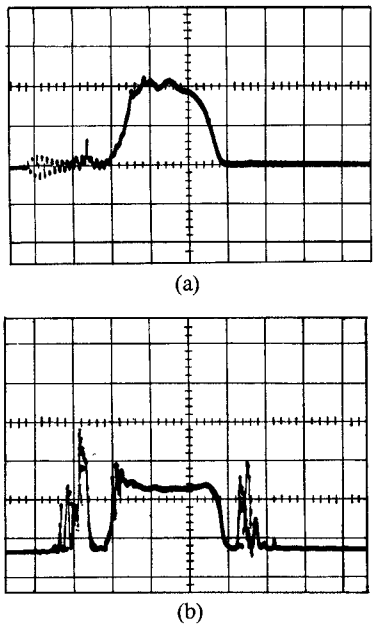

Fig. 2. Examples of RF emission as seen by a video diode during the voltage pulse of the gyrotron. Each horizontal division corresponds to 0.5 μs. (a) Diode signal when only the TE_{031} mode is excited. (b) Signal when TE_{521} is excited during the rise and fall of the voltage, while both TE_{521} and TE_{031} oscillate simultaneously in the central flattop region, as verified by the mixer-diode system.

disadvantages of each approach are listed in the last two columns. The variables m and n are arbitrary integers. The first two rows describe ways of measuring the frequency ω of the input radiation. In a fundamental mixer, an LO signal is inputted with a frequency ω_{LO} comparable to ω. If the IF filter has a narrow bandwidth, and ω_{LO} is well known, then ω can be accurately determined. Unfortunately, LO sources become less available and quite expensive at high frequencies. One way to circumvent this problem is to use a harmonic mixer, as shown on the second line. Then ω_{LO} can be reduced by a factor of n. The primary disadvantage with this approach is the higher conversion losses typically associated with harmonic mixers, thus requiring higher input power.

As a result of the strongly nonlinear behavior of the harmonic mixer, it will respond not only at ω, but also at $\Delta\omega = \omega_2 - \omega_1$, the beat frequency between two incoming RF signals with frequencies ω_1 and ω_2 that are present simultaneously. This leads to the techniques shown in the last two rows of the table. If the frequency difference between the two signals is small (e.g., less than 5 GHz), then operating the harmonic mixer without an LO is the best approach. In this case, there is only one arbitrary variable in the resonance condition, and therefore the data is easier to interpret. We relied primarily on this method to gather the data presented in the next section. If more sensitivity is required, or $\Delta\omega$ is large, then an LO signal will be required. With two arbitrary variables n and m, a larger number of resonance signals will be generated, making interpretation more difficult. Using these two approaches, $\Delta\omega$ in the range of 0 to 12.4 GHz was measured. To ensure that the system was operating correctly, the wavemeter was used to absorb one of the input signals. We then verified that the IF signals corresponding to $\Delta\omega$ were not present.

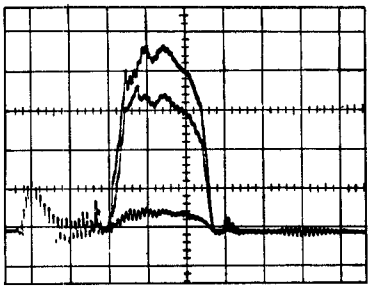

Fig. 3. An example of multimode oscillation detection using a wavemeter. Each horizontal division represents 0.5 μs. The top trace shows the video diode signal corresponding to emission of the TE_{031} (140.4 GHz) and TE_{521} (145.2 GHz) modes. The middle trace is the remaining signal after 145.2-GHz emission is absorbed by a wavemeter. The bottom trace is the remaining signal after 140.4-GHz emission is absorbed.

III. Experimental Results

The output power of the gyrotron was monitored with a fast video diode located at the maximum lobe of the far-field radiation pattern. Fig. 2(a) and (b) shows two examples of RF emission during the voltage pulse, which has a risetime of 1.5 μs and a flattop of 0.8 μs. The first trace shows the output signal when only the TE_{031} mode is excited. This requires careful tuning of the voltage and magnetic field. After some initial ringing, the TE_{031} turns on at a critical V_c, and RF power increases as the voltage rises. Mixer techniques found that no other modes were excited while the TE_{031} was present. This trace is in sharp contrast to Fig. 2(b), which is more typical of the RF output of a pulsed tube. In our power supply, the anode voltage V_a is tied to the cathode voltage via a resistive divider, so that the ratio V_a/V_c remains constant during the pulse. Theory predicts [12] that neighboring modes at higher frequency will be excited during the rise and fall of the voltage. This is evident in the trace, where the spikes at the beginning and end of the pulse correspond to the TE_{521} mode (145.2 GHz), while the central region represents the TE_{031} mode. Mixer techniques revealed that, in this particular instance, multimoding was occurring in the central region, with both the TE_{031} and TE_{521} modes oscillating simultaneously.

If the gyrotron is oscillating in two modes simultaneously, and the two signals are relatively strong, then a wavemeter can be used to confirm that multimoding is occurring. Fig. 3 shows an example of this. In this figure, three traces have been superimposed. The peak voltage and magnetic field have been kept fixed for all three pulses. The upper trace corresponds to the full output power of the gyrotron, which in this case is a combination of TE_{031} (140.4 GHz) and TE_{521} (145.2 GHz). In the middle trace, the RF at 145.2 GHz has been absorbed by the wavemeter, leaving only the TE_{031} mode. In the lower trace, the RF at 140.4 GHz has been absorbed, leaving TE_{521}. Notice that both modes appear to be excited simultaneously and that the power in the TE_{031} mode is greater than in the TE_{521} mode. Use of a wavemeter to detect multimoding is practi-

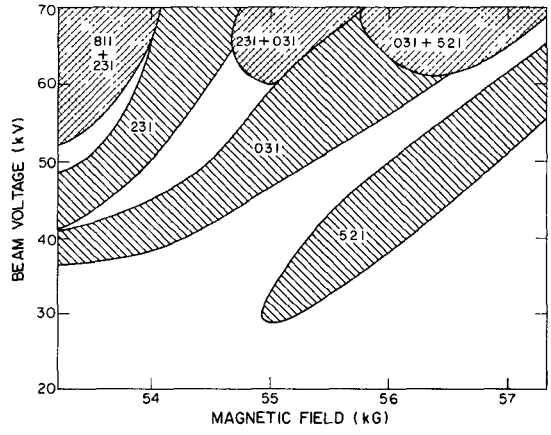

Fig. 4. Observed regions of single-mode and multimode oscillation. Data was taken at a peak beam current of 4.4 A.

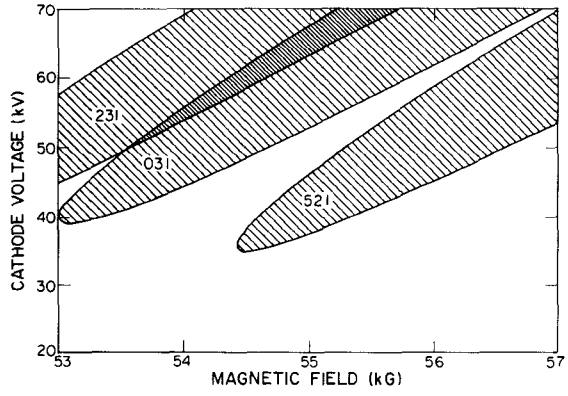

Fig. 5. Regions of single-mode excitation as predicted by linear theory. A Gaussian axial RF profile, and same device parameters as those associated with Fig. 4, were assumed.

cal in this situation where both signals are strong, but if one of the signals is weak or if $\Delta\omega$ must be known accurately, then mixing techniques must be used.

Using the diagnostic techniques described in the previous section, a map of the modes excited in the gyrotron has been produced. The results are shown in Fig. 4, where regions of single-mode and multimode oscillation have been plotted as a function of V_c and B_o. This experimental data was taken at a peak beam current of 4.4 A. The highest power was obtained from the device at 70 kV in a range of magnetic field of 53.4–58 kG, corresponding to the excitation of the TE_{231}, TE_{031}, and TE_{521} modes. Although the gyrotron gun is designed for optimum operation at 65 kV, the beam quality remains sufficiently good at lower voltages that modes can be excited as low as 30 kV. Multimoding tends to occur at higher voltages, in this case, above 55 kV, where the excitation regions of the modes are broader and therefore increasingly overlap. The figure indicates that an area of multimode oscillation appears between each pair of neighboring modes. Of special interest is the interaction between the TE_{031} and TE_{521} modes. An area of no oscillation separates the pure TE_{521} region from the multimode region. This suggests that the presence of TE_{031} introduces a new region in which the TE_{521} can be excited. This phenomenon is predicted by theory, as will be discussed in the next section. A final observation is the presence of the TE_{811} whispering-gallery mode at lower magnetic fields. This mode was excited at high starting currents and produced low power. Since whispering-gallery modes are located near the cavity wall, the difficulty in exciting this mode suggests that the electron beam is reasonably well centered in the resonator.

IV. Theory of Multimoding

Linear theory can be used to predict the conditions under which single modes will be excited in an empty cavity [22], [12]. However, in order to realistically model a pulsed tube, one must account for variations of V_c, V_a, and the beam current during the rise and fall of the pulse. Fig. 5 is a prediction based on linear theory of what modes should be excited in our device. This mode map was calculated based on the same operating conditions as in Fig. 4, with the beam located at the second radial maximum of the RF field, a peak current of 4.4 A, a total cavity Q of 1400, and a Gaussian axial RF field profile ($f(z) = e^{-(k_{\|}z)^2}$) with $k_{\|} = 1.31/\text{cm}$. The evolution of the beam voltage and current during the pulse was modeled after the variations measured experimentally. The perpendicular and parallel velocities of the electrons $v_\perp$ and $v_{\|}$ were assumed to vary as the gun voltages varied. They were modeled according to adiabatic theory [23], and achieved a ratio $v_\perp/v_{\|}$ of 1.5 at 65 kV and 55 kG. A comparison of Fig. 4 with Fig. 5 indicates good agreement between the single-mode experimental data and linear theory.

The slope of the mode excitation regions in Fig. 5 can be understood by noting that the Doppler-shifted resonance condition $\omega_c - \omega \simeq -k\|v\|$ must remain satisfied during the voltage and current changes at the beginning and end of the pulse in order for a mode to continue oscillating. In this equation, $\omega_c = eB_0/\gamma m_0 c$ is the cyclotron frequency, and $k_{\|} = q\pi/L$, where L is the effective cavity length. Since the term $k\|v\|$ is small for a gyrotron, and can be shown to remain relatively constant during the pulse, this resonance condition is maintained if ω_c remains fixed. If ω_c is written in terms of B_0 and V_c, then the following slope of the resonance regions can be derived:

$$\frac{\partial V_c(kV)}{\partial B_0(kG)} = \frac{511\gamma}{B_0(kG)}. \tag{1}$$

For our experiment, this yields a slope of approximately 10 kV/kG, in good agreement with both the theoretical curves in Fig. 5 and the data in Fig. 4.

In order to explain those regions where multimoding is occurring, a nonlinear description of the interaction between the beam and RF field is necessary. First one determines the equilibrium state of a mode that already exists in the cavity. Then the starting current of a parasitic mode is calculated in order to ascertain if multimode oscillations are possible. Finally, if multimoding can occur, then the final equilibrium states of the two modes must be determined. In the following section, the derivation of the starting current of a parasitic mode utilizing the method of

successive approximations will be presented. This methodology was first applied to the problem of multimoding in gyrotrons by Nusinovich [10]. This technique can also be used to determine the final equilibrium states of the modes, but in this paper we will restrict our attention to the calculation of the starting current.

For a gyrotron operating at the fundamental ($\omega \simeq \omega_c$), the dynamics of the interaction of the beam and RF field are governed by the following equations [11]:

$$\frac{dF_s}{d\tau} = \left(\Phi_s' - \frac{1}{2Q_s}\right)F_s \tag{2}$$

$$\frac{d\Psi_s}{d\tau} = \Phi_s'' + \frac{\omega_s}{\omega_{co}} - 1 \tag{3}$$

where F_s is a function of the field amplitude of mode s, and Ψ_s is the relative phase of the field to the cyclotron motion of an unperturbed electron (i.e., an electron orbiting at a frequency ω_{c0}). Each mode is characterized by a resonator frequency ω_s and a total cavity Q_s. Time is represented by the normalized parameter $\tau = \omega_{c0}t$. If a TE mode in a cylindrical cavity with a rotating azimuthal structure and an amplitude E_s is assumed, then F_s can be written as

$$F_s = \frac{2E_s}{B_0\beta_{\perp 0}^3} J_{m_s \pm 1}\left(\frac{2\pi R_e}{\lambda}\right) \tag{4}$$

where $\beta_{\perp 0}$ is the initial value of $v_\perp/c$, R_e is the beam radius, and the choice of sign depends on the direction of rotation of the mode.

The variable $\Phi_s = \Phi_s' + i\Phi_s''$ characterizes the interaction between the beam and mode s. The imaginary component Φ_s'' corresponds to the frequency pulling by the beam. This term scales as $1/Q_s$ and can generally be neglected in (3), leading to the result that Ψ_s varies linearly with time. The real component of Φ_s, Φ_s', describes the energy transfer between the RF field and beam. When this variable is positive, there is a net transfer of energy from the beam to the field. In (2), this term is offset by the loss mechanisms, which are represented by $1/2Q_s$ and include ohmic and diffractive losses. An equilibrium is reached (i.e., $dF_s/d\tau = 0$) when $\Phi_s' = 1/2Q_s$.

Two assumptions will be made in order to simplify the multimode analysis. First, in order that a steady state is achieved, it will be assumed that $\Delta\omega/\omega \gg 2\pi/Q$. Otherwise, it can be shown [15] that if two modes are present, their combined RF field will tend to oscillate in amplitude at the beat frequency $\Delta\omega$. The second assumption will be that m_1 and m_2 are not equal (again restricting our attention to the fundamental interaction). In this case, one can prove [11], [13] that the dynamics of the gyrotron will not depend on the phases of the modes, only on their amplitudes.

Using the method of successive approximations, one can expand Φ_s in terms of powers of the field amplitudes of the two interacting modes. In the discussion that follows, the subscript 1 will be used to refer to the mode that is already oscillating in the gyrotron, while the subscript 2 will represent the parasitic mode. Therefore, Φ_1 represents the interaction of mode 1 with an electron beam perturbed by both modes 1 and 2. Mathematically, this can be expressed as

$$\Phi_1 = I_1\left[a(x_1) - \beta(x_1)F_1^2 - \gamma(x_1, x_2)F_2^2 + \cdots\right] \tag{5}$$

where $x_s = (\omega_{c0} - \omega_s)/k\|v\|$ is the detuning parameter, and I_s is a parameter proportional to the beam current

$$I_s = \frac{0.12\times 10^{-3} I(A)\left[J_{m_s\pm 1}\left(\frac{2\pi R_e}{\lambda}\right)\right]^2}{\beta_{\perp 0}^2\beta_{\|0}\gamma_0 J_{m_s}^2(\nu_{m_s p_s})\left(\nu_{m_s p_s}^2 - m_s^2\right)\int_0^{\bar{L}}|f_s|^2\,d\bar{z}}. \tag{6}$$

In this equation, f_s is the axial profile of the RF field, $\bar{z} = \beta_{\perp 0}^2\omega_{c0}z/2v_{\|0}$ is the normalized axial coordinate, and $\bar{L} = \beta_{\perp 0}^2\omega_{c0}L/2v_{\|0}$ is the normalized length of the cavity. In order to determine the equilibrium conditions, one must calculate the coefficients α, β, and γ, which depend on the axial RF field. It should be noted F_s and I_s are real variables, while the coefficients are complex. Therefore, in calculating Φ_s', the real components of these coefficients must be determined.

Using the above equation, the starting current for mode 1 with no parasitic mode present can be calculated by setting $F_1 = F_2 = 0$ in the equilibrium condition. This leads to the following expression:

$$I_1 = \frac{1}{2Q_1\alpha'(x_1)} \tag{7}$$

where a prime indicates the real component of a variable. Once mode 1 is excited, a new equilibrium is established with $F_1 > 0$. In order to simplify this analysis, the assumption will be made that mode 1 is excited in the "soft excitation region." This is the region of parameter space in which the gyrotron will not oscillate unless the beam current exceeds the starting current. The limits of this region can be defined approximately as $-1 < x_1 < 0$ for $q = 1$ modes. Previous work [11] has shown that, in the soft excitation region, only terms up to F_1^2 are required to describe the nonlinear evolution of the mode. Therefore, keeping only the first two terms in the expansion of (5), the amplitude of mode 1 when stable equilibrium is reached is

$$F_1 = \sqrt{\frac{1}{\beta'(x_1)}\left(\alpha'(x_1) - \frac{1}{2I_1Q_1}\right)}. \tag{8}$$

Using this value of F_1, it is possible to obtain an expression for $\eta_\perp$, the efficiency of energy transfer from the perpendicular energy of the electrons to the RF field. For a cavity in equilibrium, this efficiency can be defined as $\eta_\perp = F_1^2/(I_1Q_1)$. Substituting (8) into this definition leads to the following result:

$$\eta_\perp = \frac{\alpha'(x_1) - \frac{1}{2I_1Q_1}}{\beta'(x_1)I_1Q_1}. \tag{9}$$

For a given axial RF profile, and fixed values of x_1 and $\bar{L}$, I_1Q_1 can be varied (e.g., by varying the beam current) until a maximum efficiency is obtained. This maximum occurs

at $I_1Q_1 = 1/\alpha'(x_1)$ and can be written as

$$\eta_{\perp}^{\max} = \frac{\alpha'^2(x_1)}{2\beta'(x_1)}. \tag{10}$$

Again, it should be stressed that these results are valid for values of x between 0 and -1. A gyrotron oscillating in a $q=1$ mode typically achieves its highest efficiency when operating in what is known as the "hard excitation region," with values of $x < -1$. In order to analyze this region of operation, an additional term proportional to F_1^4 is required in the expansion of Φ_1 (5), which leads to a new expression for the amplitude F_1.

To find those regions where parasitic modes are excited when mode 1 is present, one must determine Φ_2 for $F_1 > 0$ and $F_2 = 0$. Using the expression for F_1 as given by (8), the starting current for mode 2 can be written as

$$I_2 = \frac{1}{2Q_2\left(\alpha'(x_2) - \gamma'(x_2, x_1)F_1^2\right)} \tag{11}$$

$$= \frac{1}{2Q_2\left[\alpha'(x_2) - \dfrac{\gamma'(x_2, x_1)}{\beta'(x_1)}\left(\alpha'(x_1) - \dfrac{1}{2I_1Q_1}\right)\right]}. \tag{12}$$

In these equations, the first term in the denominator is the linear component of the expansion in (5), while the second term represents coupling between the modes. If $\gamma' > 0$, then mode 2 is suppressed by mode 1. However, if $\gamma' < 0$, then the region in which the parasitic mode can be excited will be enlarged by the presence of the first mode. This latter situation will be referred to as "mode enhancement."

We have analytically calculated the coefficients α, β, and γ for a flat axial field profile: $f(\bar{z}) = 1/\bar{L}$ for $0 \leqslant \bar{z} \leqslant \bar{L}$. If $\bar{L} \gg 1$ is assumed, then the following expressions are obtained:

$$\alpha'(\theta) = -\bar{L}\theta^{-3}\left[\theta\sin(\theta) + 2(\cos(\theta) - 1)\right] \tag{13}$$

$$\beta'(\theta) = \frac{\bar{L}^3}{2}\theta^{-7}\left[11\theta\sin(2\theta) + (18 - 2\theta^2)\cos(2\theta) + (53\theta - \theta^3)\sin(\theta) + (48 - 13\theta^2)\cos(\theta) - 66\right] \tag{14}$$

$$\simeq 6.55 \times 10^{-3}\bar{L}^3\sin(0.92\theta) \tag{15}$$

where $\theta = -\pi q x$ is the detuning variable as defined by Nusinovich. Equation (15) is a fitted expression for β that is accurate in the soft excitation region $0 \leqslant \theta \leqslant \pi$. The assumption $\bar{L} \gg 1$ is equivalent to saying that the gain resulting from the relativistic bunching mechanism is much stronger than the absorption mechanism, and therefore the absorption terms can be neglected. The expression for the coupling coefficient γ is quite long and is not given here. However, plots of all three coefficients can be found in the Nusinovich article on gyrotron mode behavior [10].

In order to confirm the accuracy of these results, the efficiency as given by (9) has been compared with numerical predictions based on a computer code that simulates the nonlinear beam-wave interaction in a gyrotron. This code has verified the accuracy of (9) within the constraints discussed in this section.

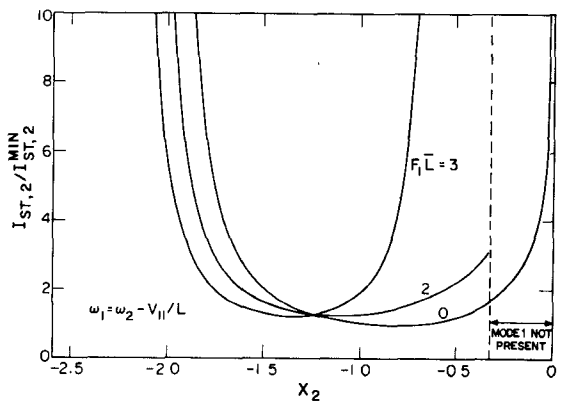

Fig. 6. A plot of the starting current of a parasitic mode (mode 2) for various amplitudes of a mode (mode 1) already present in the cavity. The starting current has been normalized to its minimum value.

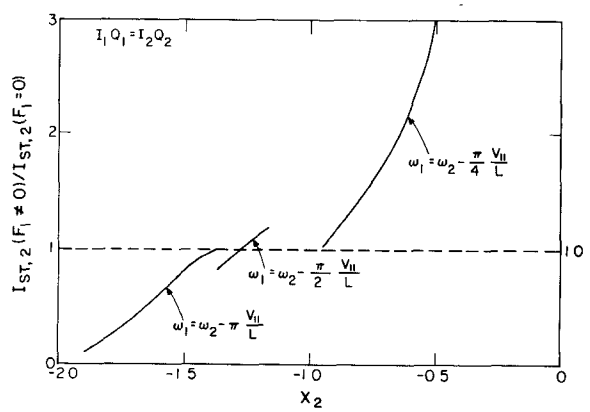

Fig. 7. A plot of the starting current of a parasitic mode (mode 2) for various values of ω_1. The starting current is normalized to the current required for excitation if mode 1 were not present. Results above the dotted line represent mode suppression, while those below correspond to mode enhancement.

The effect of γ on the starting current of mode 2, $I_{ST,2}$, can be seen in Fig. 6. In this plot $I_{ST,2}$, which has been normalized to its minimum value, is plotted versus the detuning parameter x_2 for various values of $F_1\bar{L}$. These curves are valid for all cavity lengths consistent with the assumption $\bar{L} \gg 1$. The $F_1\bar{L} = 0$ curve corresponds to the results based on linear theory. One can see that, as the amplitude of mode 1 increases, mode suppression occurs at higher values of x_2, while mode enhancement occurs at lower values. The net result is that the width of the excitation region decreases somewhat and the region shifts to lower values of x_2, that is, to lower magnetic fields.

In actuality, F_1 is not a free variable but is determined by (8). The effect of including this equilibrium value for F_1 is shown in Fig. 7. In this figure, $I_{ST,2}$ $(F_1 \neq 0)$ represents the current needed to excite mode 2 when mode 1 is present. In essence, it is the current required for multimode oscillations to be initiated. $I_{ST,2}$ has been normalized to the expected starting current if mode 1 were not present. As a result, ratios above the dotted line correspond to mode suppression, while those below correspond to mode en-

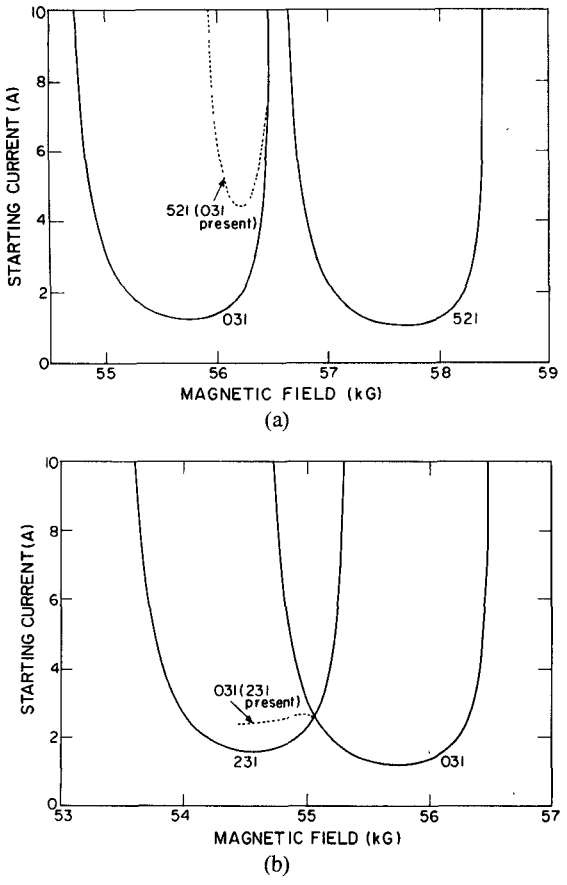

Fig. 8. The starting current required to excite various modes in the 140-GHz gyrotron. Solid lines indicate regions of single-mode excitation, while dotted lines delineate regions of multimoding. (a) TE_{031} and TE_{521} modes, (b) TE_{231} and TE_{031} modes.

hancement. Curves are shown for three values of ω_1, and it is assumed that both modes have the same value of $I_s Q_s$. This figure indicates that if the frequencies of the two modes are closer than the gain bandwidth $\pi v_{\|}/L$, then mode 1 will tend to suppress mode 2. However, when ω_2 is greater than ω_1 by approximately the gain bandwidth, then enhancement of mode 2 predominates. This enhancement effect can be quite strong, and under certain circumstances mode 2 will be excited only if mode 1 is present. Physically, mode enhancement occurs because mode 1 is able to prebunch the beam so that it interacts favorably with mode 2.

This theoretical model of gyrotron mode behavior has been utilized to analyze the multimode oscillations observed in our experiment. Using the cavity and beam characteristics as given in Section III, the starting currents of various modes have been calculated as a function of B_o. The results are shown in Fig. 8(a) for the TE_{031} and TE_{521} modes, and in Fig. 8(b) for TE_{031} and TE_{231}. These calculations assume a beam voltage fixed at a final value of 65 kV, and therefore do not describe the behavior of the gyrotron during the rise and fall of the voltage pulse. The solid curves represent the starting currents when no mode is present in the resonator, while the dashed line gives I_{ST} when the indicated mode is present, and therefore delineates the region where multimoding occurs. Note that in Fig. 8(b) the dashed line ends abruptly because the TE_{231} mode is no longer in the soft excitation region, and therefore the theory outlined above is no longer valid. Comparing these theoretical results with the experimental data at 65 kV in Fig. 4 indicates good agreement. In both cases, the currents needed to initiate multimoding are comparable. In addition, theory predicts the existence of a gap between the single-mode TE_{521} region and the multimode TE_{031}/TE_{521} region, as is seen experimentally. No such gap exists in the case of the TE_{031} and TE_{231} modes, as both theory and experiment indicate.

Another potential source of multimode oscillations in gyrotrons is the radial spread of the electron beam. This is particularly problematic in high-frequency devices in which $\Delta R_e/R_g$, the ratio of the beam thickness to the Larmor radius, becomes relatively large. Most past studies of multimoding have assumed a thin beam, and therefore have not predicted this effect. Using adiabatic theory, we have related the thickness of the beam in the resonator to its width at the cathode. Based on this result, the following expression was obtained [24]:

$$\frac{\Delta R_e}{R_g} = 2 + \frac{2\pi I \sin\theta}{\beta_\perp \alpha \lambda^2 v_{m-1,s} J_k} \tag{16}$$

where θ is the angle of the cathode surface with respect to the axis of the gun, α is the ratio of magnetic field at the cavity to that at the gun, J_k is the cathode emission current density, and it is assumed that the beam interacts with the sth radial maximum of the TE_{mpq} mode. As a result of the λ^2 dependence in the above equation, the beams in high-frequency gyrotrons are typically relatively thick. If the cavity is oversized and can support many modes, it may be possible for different radial parts of the beam to interact with and excite different modes, thus leading to multimoding. This phenomenon is similar to spatial hole burning in lasers [25], except in this case the active medium is the beam rather than a gas. This effect can also occur for modes having different azimuthal structures.

In Fig. 9(a) through (c), the strength of the coupling in a gyrotron between the beam and various competing TE modes has been plotted as a function of the beam radius R_e. Using linear theory [22], one can show that this coupling is proportional to $J_{m\pm1}^2(2\pi R_e/\lambda)$. In these graphs, the beam radius has been normalized to the cavity radius R_o while the coupling strength has been normalized to the stored energy in the cavity. Note that for modes with $m > 0$ there are two branches, designated by + and −, where the choice of sign depends on the direction of azimuthal rotation of the mode. Also shown in these figures is the theoretical location and width of an electron beam designed to interact with the second radial maximum of the TE_{031} mode. Fig. 9(a) and (b) indicates that at the second maximum it is virtually impossible to use the radial position of the beam to avoid coupling with a neighboring mode of the TE_{031}. Peaks of the negative branches of both the TE_{231} and TE_{521} modes coincide with the peak of the TE_{031}. Only surface modes, such as the whispering-gallery TE_{811} mode shown in Fig. 9(c), will weakly couple to the

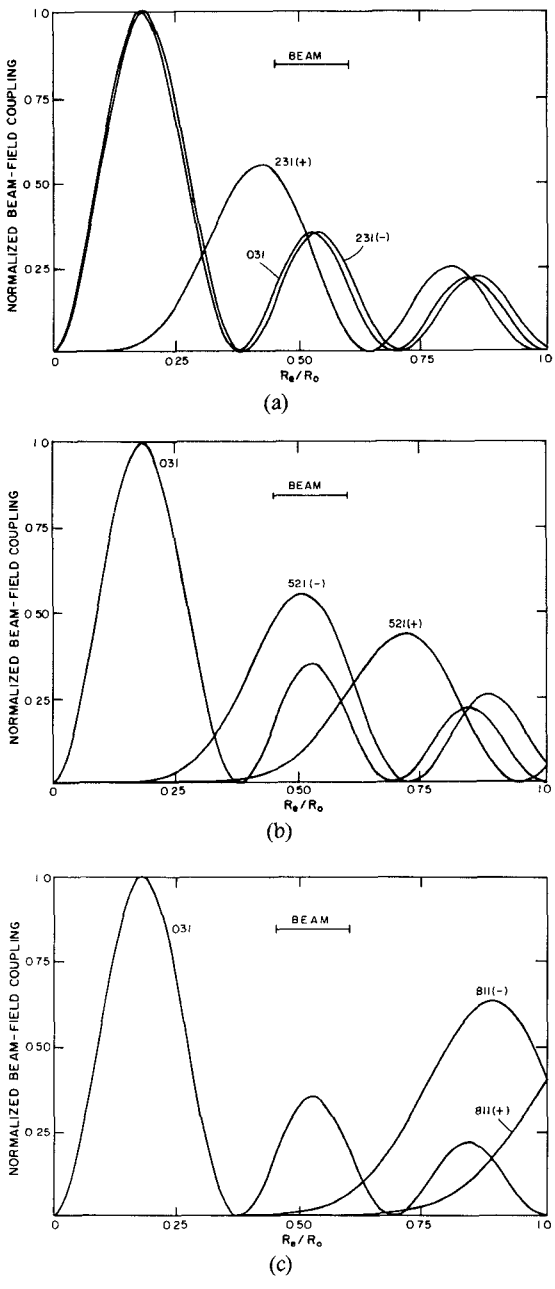

Fig. 9. The coupling strength between the electron beam and various modes in a gyrotron. The coupling strength has been normalized to the stored energy of the mode. Also shown is the actual location of the beam in our device. The + and − signs indicate the direction of azimuthal rotation of the mode. (a) TE_{031} and TE_{231}, (b) TE_{031} and TE_{521}, (c) TE_{031} and TE_{811}.

beam. These figures illustrate the severity of the problem of mode competition in high-power, high-frequency gyrotrons. Due to space-charge effects resulting from high current densities and small cavity dimensions, it will become necessary for the beam to be located away from the cavity center, and as a result it will not be able to interact with the innermost radial maximum. The beam therefore will be capable of coupling to a large number of asymmetric modes. If the spatial location of the beam is to be used as a mode-selection technique in such a device, then the most promising approach is to locate the beam near the cavity wall where only the whispering-gallery modes are strong.

These figures also show how a beam with a finite thickness can lead to multimoding. For example, if the beam in Fig. 9(a) had a smaller radius, then the inner part of the beam could excite the $TE_{231}(+)$ mode, while the outer part excited either the TE_{031} or the $TE_{231}(-)$ mode. Even if the beam were thinner, such an effect could occur if it were misaligned in the cavity. Then, the radial position of the beam would vary as one moved azimuthally, and different azimuthal parts of the beam could couple with different modes. It is therefore important when trying to understand mode behavior in high-frequency gyrotrons to model the beam realistically, and include such characteristics as radial thickness and the possibility of misalignment.

A comparison of experimental data with theory suggests that mode enhancement rather than beam thickness is the predominant cause of multimode oscillations in our device. This conclusion is primarily based on the existence of a gap between the TE_{031} and TE_{521} modes (see Fig. 4). If beam thickness were the sole cause of multimoding in our gyrotron, then one would expect multimode oscillations to occur only when the excitation regions of neighboring modes overlap. The experimental observation of a gap between the TE_{031} and TE_{521} modes indicates that their excitation regions do not overlap, yet multimoding is observed. Further evidence supporting mode enhancement as the cause of multimoding is the similarity between the data of Fig. 4 and the theory shown in Fig. 8(a).

V. Conclusions

In this paper, an extensive study of mode competition and multimode oscillations in a 140-GHz gyrotron has been described. The development of an understanding of mode behavior in high-frequency gyrotrons becomes important as these devices are scaled to higher powers and CW operation. In order to avoid low efficiency due to multimoding and excessive heating of components by parasitic modes, it is necessary to develop practical techniques that allow one to excite the mode of interest and maintain single-mode oscillation during the entire pulse. This becomes more difficult as the resonator increases in size to accommodate higher powers and, as a result, becomes highly overmoded. The evaluation of the effectiveness of various mode suppression techniques requires a good understanding of the interaction between the beam and RF field, and the development of reliable diagnostic methods that allow one to analyze the performance of the device.

A variety of mixer-diode techniques have been used to study mode behavior in our gyrotron. To our knowledge, this is the first use of mixing techniques in conjunction with the study of gyrotron operation. A summary of these diagnostic methods is given in Table I, including their advantages and disadvantages. It was found that, as a result of the strongly nonlinear characteristics of a harmonic mixer, an IF signal was produced corresponding to the frequency difference $\Delta\omega$ of two modes simultaneously present. This diode therefore could be used to conclusively verify the presence of multimoding, even when one of the

RF signals is weak. A mixer system was assembled that was capable of measuring $\Delta\omega$ in the range of 0 to 12.4 GHz, and a map was produced showing regions of single-mode and multimode oscillations plotted as a function of magnetic field and cathode voltage. In some cases, when both signals were strong, a wavemeter could be used to verify that multimode oscillations were present. However, this technique is limited because of its lack of sensitivity and inability to measure $\Delta\omega$ to high accuracy. A wavemeter also cannot discriminate easily between true, simultaneous oscillations and a two-mode oscillation involving rapid switching between modes.

As a result of the high mode density in our gyrotron, it was difficult to initiate oscillation in the mode of interest and maintain single-mode emission. This could only be done at lower power and involved careful tuning of the magnetic field and cathode voltage. Typically, higher frequency modes would be excited during the rise and fall of the voltage pulse. This behavior is in part a result of the characteristics of our power supply, in which the anode voltage V_a is tied to the cathode voltage V_c via a resistive divider so that V_a/V_c remains constant during the pulse. The regions of single-mode oscillation were found to agree reasonably well with predictions based on the linear theory of pulsed gyrotrons [12] (see Figs. 4 and 5). Although the gun was designed for optimum operation at 65 kV, the beam quality remains sufficiently good at lower voltages that modes could be excited as low as 30 kV.

Although linear theory is adequate for determining the conditions leading to single-mode excitation, a nonlinear model is required to explain those regions seen in Fig. 4 where multimode oscillations occur. Using the method of successive approximation, a technique first applied to the problem of multimoding in gyrotrons by Nusinovich [9], an expression was derived for the equilibrium amplitude of a mode when the gyrotron is operating in the soft excitation region ($-1 \leqslant x \leqslant 0$). From this, a simple expression was obtained for the optimum efficiency and the conditions required to achieve this efficiency (see (10)). An expression was also derived for the starting current of a parasitic mode (mode 2) when another mode (mode 1) is already oscillating in the cavity. It was found, assuming a flat RF axial profile, that both regions of mode suppression ($I_{ST,2}(F_1 > 0) > I_{ST,2}(F_1 = 0)$) and mode enhancement ($I_{ST,2}(F_1 > 0) < I_{ST,2}(F_1 = 0)$) exist. Mode enhancement predominates when the parasitic mode has a frequency of $\omega_2 \simeq \omega_1 + \pi v_{\|}/L$, where L is the effective cavity length. In this case, mode 1 favorably prebunches the beam for excitation of mode 2. If the parasitic mode has a lower frequency than mode 1, then mode suppression occurs. A comparison of experimental data with theory suggests that mode enhancement is the mechanism leading to multimoding in our device. The best evidence supporting this conclusion is the existence of a gap between the TE_{521} single-mode region and the TE_{031}/TE_{521} multimode region, which is predicted by theory and observed experimentally.

Another potential source of multimoding and parasitic mode oscillations is the radial thickness of the electron beam. It can be shown (see (16)) that its relative thickness increases as gyrotrons are scaled to higher frequencies. Multimode oscillations can occur if different parts of the beam excite different modes. This can occur not only if the beam is thick but also if it is misaligned. The potential for this type of multimoding to occur is particularly great in high-power, high-frequency devices operating in symmetric ($m = 0$) modes. In this case the beam, in order to avoid space charge effects, will be unable to interact with the innermost radial peak and will have to be located at a peak closer to the cavity wall. It will be capable therefore of coupling to a large variety of asymmetric modes. It thus becomes important in trying to understand mode behavior in high-power, high-frequency gyrotrons to model the beam realistically, and not treat it as a thin, centered beam.

ACKNOWLEDGMENT

We wish to thank K. R. Chu at the Naval Research Laboratory for providing us with a copy of his nonlinear gyrotron code, and J. Schutkeker for getting the code operational and providing numerical data that allowed us to check the multimode theory. We also thank S. MacCabe for his assistance during operation of the gyrotron. Finally, we thank D. R. Cohn for his encouragement and support throughout this work.

REFERENCES

[1] H. Jory, S. Evans, J. Moran, J. Shively, D. Stone, and G. Thomas, "200 kW pulsed and CW gyrotrons at 28 GHz," in *IEDM Tech. Dig.*, 1980, paper 12.1, pp. 304–307.

[2] G. Mourier, G. Boucher, P. Boulanger, P. Charbit, G. Faillon, A Herscovici, and E. Kammerer, "A gyrotron study program," in *Sixth Int. Conf. on Infrared and Millimeter Waves Dig.*, 1981, IEEE Catalog no. 81CH1645-1 MTT.

[3] M. E. Read, R. M. Gilgenbach, R. F. Lucey, Jr., K. R. Chu, A. T. Drobot, and V. L. Granatstein, "Spatial and temporal coherence of a 35 GHz gyromonotron using the TE_{01} circular mode," *IEEE Trans. Microwave Theory Tech.*, vol. MTT-28, pp. 875–878, 1980.

[4] A. A. Andronov, V. A. Flyagin, A. V. Gaponov, A. L. Gol'denberg, M. I. Petelin, V. G. Usov, and V. K. Yulpatov, "The gyrotron: High-power source of millimetre and sub-millimetre waves," *Infrared Phys.*, vol. 18, pp. 385–393, 1978.

[5] H. Jory, S. Evans, K. Felch, J. Shively, and S. Spang, "Gyrotron oscillators for fusion heating," in *Proc. Symp. on Heating in Toroidal Plasmas*, (Grenoble), 1982.

[6] J. J. Tancredi, presented at Sixth Int. Conf. on Infrared and Millimeter Waves, Miami, 1981.

[7] A. V. Gaponov, V. A. Flyagin, A. L. Gol'denberg, G. S. Nusinovich, Sh. E. Tsimring, V. G. Usov, and S. N. Vlasov, "Powerful millimetre-wave gyrotrons," *Int. J. Electron.*, vol. 51, pp. 277–302, 1981.

[8] R. J. Temkin, K. E. Kreischer, W. J. Mulligan, S. MacCabe, and H. R. Fetterman, "A 100 kW, 140 GHz pulsed gyrotron," *Int. J. Infrared Millimeter Waves*, vol. 3, pp. 427–437, 1982.

[9] G. S. Nusinovich, "Multimoding in cyclotron-resonance masers," *Radiophys. Quantum Elect.*, vol. 19, pp. 1301–1306, 1976.

[10] G. S. Nusinovich, "Mode interaction in gyrotrons," *Int. J. Electron.*, vol. 51, pp. 457–474, 1981.

[11] M. A. Moiseev and G. S. Nusinovich, "Concerning the theory of multimode oscillation in a gyromonotron," *Radiophys. Quantum Elect.*, vol. 17, pp. 1305–1311, 1974.

[12] K. E. Kreischer and R. J. Temkin, "Mode excitation in a gyrotron operating at the fundamental," *Int. J. Infrared Millimeter Waves*, vol. 2, pp. 175–196, 1981.

[13] D. Dialetis and K. R. Chu, "Mode competition and stability analysis of the gyrotron oscillator," in *Infrared and Millimeter Waves*, vol. 7. New York: Academic Press, 1983, pp. 537–581.

[14] G. S. Nusinovich, "Mode competition in a gyromonotron with a

distorted axial symmetry," *Radio Eng. Electronic Phys.*, vol. 19, pp. 152–155, 1974.
[15] J. L. Vomvoridis, "Self-consistent nonlinear analysis of overmoded gyrotron oscillators," *Int. J. Infrared Millimeter Waves*, vol. 3, pp. 339–366, 1982.
[16] S. N. Vlasov, G. M. Zhislin, I. M. Orlova, M. I. Petelin, and G. G. Rogacheva, "Irregular waveguides as open resonators," *Radiophys. Quantum Elect.*, vol. 12, pp. 972–978, 1969.
[17] V. Ye. Zapevalov, G. S. Korablev, and S. Y. Tsimring, "An experimental investigation of a gyrotron operating at the second harmonic of the cyclotron frequency with an optimized distribution of the high-frequency field," *Radio Eng. Electronic Phys.*, vol. 22, pp. 86–94, 1977.
[18] A. K. Ganguly and K. R. Chu, "Analysis of two-cavity gyroklystron," *Int. J. Electronics*, vol. 51, pp. 503–520, 1981.
[19] A. A. Kurayev, F. G. Shevchenko, and V. P. Shestakovich, "Efficiency-optimized output cavity profiles that provide a higher margin of gyroklystron stability," *Radio Eng. Electronic Phys.*, vol. 19, pp. 96–103, 1974.
[20] Y. Carmel, K. R. Chu, D. Dialetis, A. Fliflet, M. R. Read, K. J. Kim, B. Arfin, and V. L. Granatstein, "Mode competition, suppression, and efficiency enhancement in overmoded gyrotron oscillators," *Int. J. Infrared Millimeter Waves*, vol. 3, pp. 645–665, 1982.
[21] H. R. Fetterman, P. E. Tannenwald, B. J. Clifton, C. D. Parker, W. D. Fitzgerald, and N. R. Erickson, "Far-IR heterodyne radiometric measurements with quasioptical Schottky diode mixers," *Appl. Phys. Lett.*, vol. 33, pp. 151–154, 1978.
[22] K. E. Kreischer and R. J. Temkin, "Linear theory of an electron cyclotron maser operating at the fundamental," *Int. J. Infrared Millimeter Waves*, vol. 1, pp. 195–223, 1980.
[23] K. E. Kreischer and R. J. Temkin, "High frequency gyrotrons and their applications to tokamak plasma heating," in *Infrared and Millimeter Waves*, vol. 7. New York: Academic Press, 1983, Appen. C, pp. 377–385.
[24] K. Felch, D. Stone, H. Jory, R. Garcia, G. Wendell, R. J. Temkin, and K. E. Kreischer, "Design and operation of magnetron injection guns for a 140 GHz gyrotron," in *IEDM Tech. Dig.*, 1982, paper 14.1, pp. 362–365.
[25] P. W. Smith, "Mode selection in lasers," *Proc. IEEE*, vol. 60, pp. 422–440, 1972.

✤

Kenneth E. Kreischer was born in Aberdeen, MD, on August 30, 1954. He received both the B.S. degree in physics and the M.S. degree in nuclear engineering in 1977 from the Massachusetts Institute of Technology, Cambridge. In 1981, he received the Ph.D. degree in nuclear engineering, also from MIT. His doctoral thesis was a theoretical study of high-frequency (100–200 GHz) gyrotrons and their applicability to heating fusion tokamak reactors.

He has remained at MIT since 1981 as a Research Scientist for the fusion systems division of the Plasma Fusion Center. He has been involved in the design and construction of a high-power, 140-GHz gyrotron, which became operational in early 1982. He is presently responsible for its operation and has developed a variety of diagnostic techniques that have been used to analyze its performance.

Dr. Kreischer is a member of Sigma Xi and Phi Beta Kappa.

Richard J. Temkin was born in Boston, MA, on January 18, 1945. He received the B.S. degree from Harvard University, Cambridge, MA, in 1966, and the Ph.D. degree in physics from the Massachusetts Institute of Technology, Cambridge, in 1971.

From 1971 to 1974, he was a Research Fellow in the Division of Engineering and Applied Physics of Harvard University. From 1974 to 1979, he was a staff member of the Francis Bitter National Magnet Laboratory at the Massachusetts Institute of Technology, Since 1980, he has been a group leader of the Gyrotron and Advanced Millimeter Sources Group of the Massachusetts Institute of Technology Plasma Fusion Center and a member of the Alcator Tokamak Group. His current research interests include: electron-cyclotron masers (gyrotrons), plasma heating and diagnostics at electron cyclotron resonance, and infrared and far infrared laser-pumped molecular lasers.

Dr. Temkin is a member of the American Physical Society.

✤

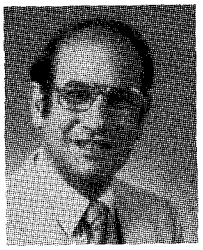

Harold R. Fetterman (SM'81) was born in Jamaica, NY, on January 17, 1941. He received the B.A. degree in physics from Brandeis University Waltham, MA, and the Ph.D. degree from Cornell University, Ithaca, NY.

After 13 years in the Solid State Research Division of Lincoln Laboratory MIT, he joined the Electrical Engineering Department of UCLA as a Professor in 1982. At UCLA, he is active in the newly formed "Millimeter Wave and High Frequency Electronics Center."

Professor Fetterman is a Fellow of the OSA, a member of Sigma Xi and the APS, and a founder of the MilliTech Corporation of Amherst, MA.

✤

William J. Mulligan was born in County Mayo, Ireland, on February 7, 1925. He received the A.E. degree in electronics and the B.B.A. degree in engineering and management from Northeastern University, Boston, MA, in 1957 and 1959, respectively.

From 1956 to 1976, he worked at the Research Laboratory of Electronics, Massachusetts Institute of Technology, Cambridge, where he designed and fabricated electronic and high-voltage equipment as related to plasma physics and lasers. In 1976, he joined the Plasma Fusion Center, Massachusetts Institute of Technology, Cambridge, where he is currently a Technical Staff Member involved in submillimeter laser and gyrotron research and development.